The effects of interparticle forces on the stability of gas-fluidized beds. II. Theoretical derivation of bed elasticity on the basis of van der Waals forces between powder particles

Please check the document version of this publication:

• A submitted manuscript is the version of the article upon submission and before peer-review. There can be important differences between the submitted version and the official published version of record. People interested in the research are advised to contact the author for the final version of the publication, or visit the DOI to the publisher's website.
• The final author version and the galley proof are versions of the publication after peer review.
• The final published version features the final layout of the paper including the volume, issue and page numbers.

[Link to publication](#)

THE EFFECT OF INTERPARTICLE FORCES ON THE STABILITY OF GAS-FLUIDIZED BEDS—II. THEORETICAL DERIVATION OF BED ELASTICITY ON THE BASIS OF VAN DER WAALS FORCES BETWEEN POWDER PARTICLES

K. RIETEMA, E. J. E. COTTAAR and H. W. PIEPERS†

Department of Chemical Engineering, Eindhoven University of Technology, Eindhoven,
The Netherlands

Abstract—In Part I of this series it was shown, on the basis of elasticity of the bed structure, that a fluidized powder bed can be stable. It was also suggested that the origin of the elasticity is to be found in the existence of interparticle forces. These interparticle forces are the subject of the present paper. The van der Waals forces between the two neighbouring particles are discussed, while the effect of particle deformation is calculated. Starting from the interparticle forces at the asperities, a model is derived that describes the dependence of the elasticity modulus on the characteristics of the particle bed as, e.g., the bed porosity, the particle diameter and the coordination number.

INTRODUCTION

In Part I of this series (Rietema and Piepers, 1990) two experiments were discussed, on the basis of which it was concluded that a homogeneous gas-fluidized bed maintains a mechanical structure even when expanded. These experiments were:

(a) Measurement of the electrical conductivity of a fluidized bed of electrical conductive charcoal particles.
(b) Demonstration that a homogeneous fluidized bed can be tilted over a horizontal axis without breaking its mechanical structure.

As all mechanical structures have elastic properties it was suggested in Part I of this series that also a powder bed will have a certain elasticity. In an engineering approach we analysed the forces operating at and around the contact place between neighbouring particles in a fluidized bed. The outcome of this analysis was translated into a model that explains the elastic character of a fluidized bed. Already in 1971 it was shown by one of the present authors that introduction of an elastic force in the momentum equation of the dispersed particle phase could indeed explain that a fluidized powder bed can be stable, even when fluidized at not too high a gas velocity. In Part I it was shown that when this elastic force is suitably defined by means of an elasticity modulus E this modulus can be determined experimentally from the expansion of a stable homogeneously fluidized bed by

$$E = \rho_p \left[u_0 \frac{(3 - 2\varepsilon)}{\varepsilon} \right]^2 \qquad (1)$$

in which ε is the porosity of the stable bed, u_0 the superficial gas velocity, ρ_p the particle density and E the elasticity modulus.

It was also suggested that the origin of the elasticity could be found in the existence of interparticle forces. These interparticle forces are the subject of the present paper, while the relation between the interparticle forces on the one hand and the structure of the particle bed on the other hand will finally lead to a model that describes the dependence of the elasticity modulus on the characteristics of the particle bed as, e.g., the bed porosity, the particle size and the coordination number.

THE HAMAKER THEORY

Many investigators (Boehme *et al.*, 1962; Krupp, 1967; Johnson *et al.*, 1971; Dahneke, 1972; Derjaguin *et al.*, 1975; Tabor, 1977; Pollock, 1978) have occupied themselves, both theoretically and experimentally, with the forces of attraction between solid particles on the basis of the van der Waals forces between molecules. These forces were first derived theoretically by London (1937). According to this theory, the interaction energy between two molecules is given by

$$V_{ss} = -\frac{C_{ss}}{r^6} \qquad (2)$$

in which C_{ss} is the London–van der Waals constant, measured in J m⁶, which depends on the nature of the interacting molecules and r is the distance between these molecules. Although these forces operate only at extremely short range [the meaning of "short range" as used here is different from the definition of Krupp (1967) and pertains to distances relevant in classical mechanics], they can reach values many times the

†Author to whom correspondence should be addressed.

weight of the particles when this interaction energy is integrated over all molecules in two contacting particles. This was first shown by Bradley (1932) and Hamaker (1937). Integration is carried out according to

$$U_m = \int_{V_1} dn_1 \int_{V_2} V_{ss} \, dn_2 \tag{3}$$

in which n_1, n_2, V_1 and V_2 designate molecule densities and volume elements of the two interacting particles, respectively. For two perfectly spherical and rigid particles with diameters d_1 and d_2 this integration leads to

$$U_m = -\frac{A}{12z} \frac{d_1 d_2}{(d_1 + d_2)} \tag{4}$$

where A is the so-called Hamaker constant, $A = \pi^2 n_1 n_2 C_{ss}$, while z is the shortest distance between the particles. Equation (4) holds only as long as $z \ll D = d_1 d_2/(d_1 + d_2)$. This, however, is not a practical limitation.

The attractive force which now follows from eq. (4) is found by differentiation with respect to z:

$$F = \frac{\partial}{\partial z}(U_m) = \frac{AD}{12z^2}. \tag{5}$$

According to eq. (5), the attractive force F increases continuously when the distance z between the particles decreases and, in effect, goes to infinity when z goes to zero. This, of course, cannot be so in reality. Therefore, it was postulated by some investigators [see, e.g., Krupp (1967)] that there is a minimum distance z_0 at which the force is maximum. The value generally assumed for this minimum distance is 4 Å. The theory based on eq. (2) is generally called the microscopic theory. A later theory developed by Lifshitz (Lifshitz, 1956), the so-called macroscopic theory, gives the same dependence of the force on the distance but differs only by a constant factor.

CRITIQUE OF THE HAMAKER THEORY

Nevertheless, both theories are not realistic as it is not possible that the force between the particles is at a maximum while at the same time there must be equilibrium between forces; hence, the attractive force F_a must be balanced by a repulsive force F_r which originates similarly from the interaction energy between the molecules of the particles. Hence, it is reasonable to assume that this repulsive force too depends on the distance between the particles. Furthermore, when there is stability, the z-dependence of the repulsive force must be an even steeper function than the z-dependence of the attractive force. Lennard-Jones (1937) proposed on an empirical basis an extension of the interaction potential between molecules:

$$V_{ss} = C_{ss}\left[\frac{-1}{r^6} + \frac{r_{ss}^6}{2r^{12}}\right]. \tag{6}$$

In this equation r_{ss} is a characteristic distance of the molecules in the particles.

When integrated over all molecules in the particles according to the Hamaker equation (3), the total interaction potential between two identical particles is found to be

$$U_m = \frac{AD}{12z}\left[-1 + \frac{1}{420}\left(\frac{r_{ss}}{z}\right)^6\right] \tag{7}$$

or, in dimensionless notation, with $\zeta = z/r_{ss}$,

$$\chi = \frac{12U_m r_{ss}}{AD} = -\frac{1}{\zeta} + \frac{1}{420\zeta^7} \tag{8}$$

Again the net force between the particles in dimensionless notation is found by differentiation of eq. (8) with respect to ζ:

$$\Phi = \frac{12Fr_{ss}^2}{AD} = \frac{1}{\zeta^2}\left(1 - \frac{1}{60\zeta^6}\right). \tag{9}$$

In Fig. 1 the function Φ is plotted against the parameter ζ. The attractive force and the repulsive force as well as the resultant force are indicated. Figure 2 presents the potential of the total force. At point O, where $\zeta = 0.505$, the potential is at a minimum; hence, the net force F is zero. When from here the distance z between the particles is increased, the net force becomes attractive and reaches its maximum value F_c at z_m (in Fig. 2 at point M, $\zeta = 0.6368$), where the gradient of the potential is maximum. From eq. (9) it follows that this maximum value F_c is given by $\Phi = 1.85$. It corresponds to the value of the maximum cohesion between the particles.

An average value of $r_{ss} = 3.5 \times 10^{-10}$ m; hence, $z_m = 2.23 \times 10^{-10}$ m. For most solids an average value of $A = 10^{-19}$ J has been calculated [for a survey, see Visser (1972)]. With the above value of r_{ss} and with $d_1 = d_2 = 50\ \mu$m, it is found that the cohesion force between the particles $F_c = 31 \times 10^{-7}$ N. A comparison of this cohesion force with the weight of the
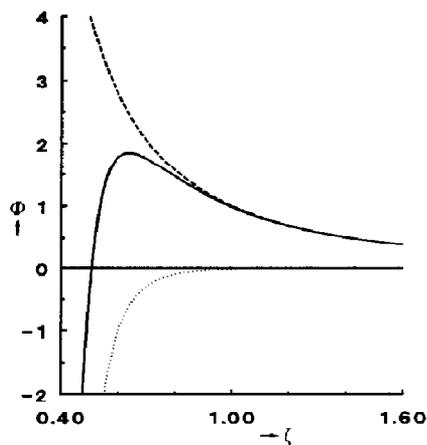

Fig. 1. Dimensionless interaction force as a function of the dimensionless particle–particle distance: (. . . . . .) repulsive force; (-----) attractive force; (———) resultant force.
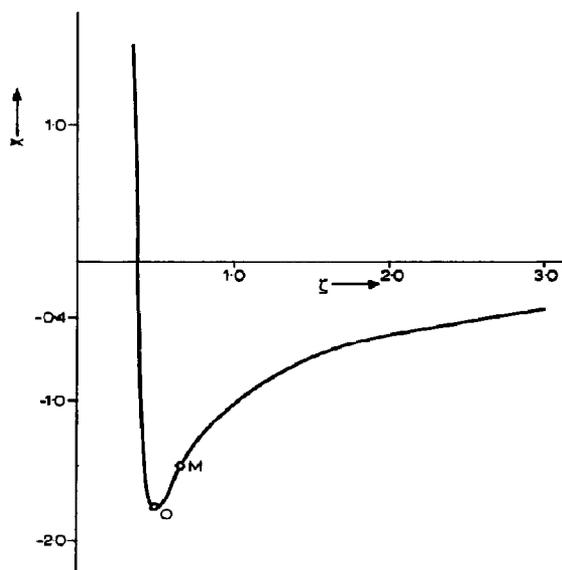
Fig. 2. Dimensionless interaction potential between two neighbouring particles based on the Lennard-Jones potential between the molecules.

particles gives for glass beads ($\rho_p = 2600\ \mathrm{kg\,m^{-3}}$): $F_c/F_{gravity} = 1900$ and for potato starch ($\rho_p = 1400\ \mathrm{kg\,m^{-3}}$): $F_c/F_{gravity} = 3600$.

These values seem to be extremely high; indeed, for potato starch, the discrete particles of which have an extremely smooth surface in comparison with most other powders (see Fig. 3), a very high cohesion can be observed which makes handling of this powder as such practically impossible. Most powders, however, have a rather rough surface with many protuberances—generally called asperities—with radii of curvature often not larger than 0.1 μm [see Donsi and Massimilla (1973) and Massimilla and Donsi (1976)]. This means that the effective contact area between the particles is determined by one, two or, at the most, three asperities. To calculate the cohesion force per asperity, not the particle diameter but the diameter of the asperities should be inserted into eq. (9). This, of course, reduces the derived cohesion force strongly. The effective average cohesion force, therefore, depends strongly on the surface structure of the particles, i.e. the size distribution of the asperities and their surface density.

EFFECT OF PARTICLE DEFORMATION

So far, we have implicitly assumed that the solid particles are rigid and will not be deformed by the forces acting upon them. Most solids, however, are not rigid and will be of different hardness. Softer particles can more easily be deformed than harder particles.

Due to the attractive forces acting upon them, the particles will be flattened over a distance h at the place

of contact with other particles or with a rigid wall. Schematically, but strongly exaggerated, this is indicated in Fig. 4 for the case of a particle in contact with a rigid wall. The theoretical analysis based on this geometry, however, holds also for the case of two contacting particles when D is interpreted as $d_1 d_2/(d_1 + d_2)$. Integration of eq. (6) over the volume of the interacting particles now results in

$$U_m = \frac{AD}{12z}\left[-\left(1 + \frac{h}{z}\right) + \frac{1}{60}\left(\frac{1}{7} + \frac{h}{z}\right)\left(\frac{r_{ss}}{z}\right)^6\right].$$
(10)

At the same time, the particles generate repulsive forces which try to compensate for the flattening. When the deformation is not too large, it will be an elastic deformation. According to Hertz (1895), the relation between the flattening h and the repulsive force is given by

$$F_r = \frac{4}{3K}\sqrt{Dh^3}$$
(11)

in which $K = (1 - v^2)/Y$, where v is Poisson's ratio and Y is Young's elasticity modulus of the solid.

The potential increase due to the flattening must also be introduced in eq. (10). This potential is found by integration of eq. (11), which gives

$$U_h = \frac{8h^{2.5}}{15K}\sqrt{D}.$$

With $\eta = h/r_{ss}$ and $\Psi = 32r_{ss}^{3.5}/5AK\sqrt{D}$, the total interaction potential is now found to be in dimensionless notation

$$\chi = -\left(\frac{1}{\zeta} + \frac{\eta}{\zeta^2}\right) + \frac{1}{60}\left(\frac{1}{7\zeta^7} + \frac{\eta}{\zeta^8}\right) + \Psi\eta^{2.5} \quad (12)$$

The distance L between the particle centre and the rigid plane now depends on two variables, viz. the distance z between the two surfaces and the flattening h of the particles: $L = R + z - h$.

Hence, the system has one degree of freedom left. At equilibrium with an external force at constant L, the potential will be at a minimum and, therefore, will not vary with z or h. Hence, at equilibrium

$$\left(\frac{dU}{dz}\right)_L = 0 \quad \text{and} \quad \left(\frac{dU}{dh}\right)_L = 0$$

or

$$\left(\frac{dU}{dz}\right)_L = \frac{\partial U}{\partial z} + \frac{\partial U}{\partial h}\left(\frac{dh}{dz}\right) = \frac{\partial U}{\partial z} + \frac{\partial U}{\partial h} = 0 \quad (13)$$

since $dh/dz = 1$ at constant L. Rewriting eq. (13) in dimensionless form and elaborating it with the help of eq. (12) results finally in

$$\sqrt{\eta} = \frac{4\zeta^{-6} - 60}{75\Psi\zeta^3}.$$
(14)

For each value of $\zeta < 0.6368$, η can be calculated. Hence, also χ can be calculated. For $\zeta > 0.6368$, $\sqrt{\eta}$ becomes negative and then it is assumed that $\eta = 0$.
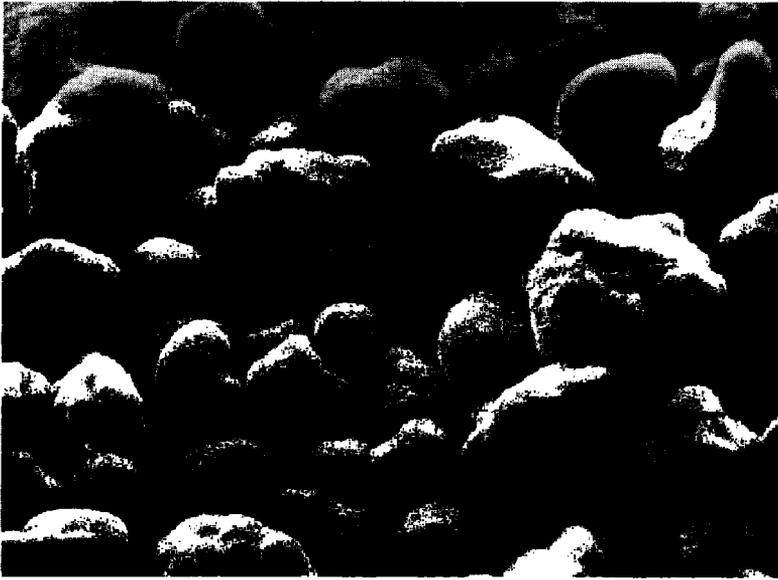
(a)

(b)

Fig. 3. (a) and (b).

Although χ has been calculated as a function of ζ, it will be plotted against $\omega = \zeta - \eta$, since ω indicates the real variation of the distance between the particles. It is the increase of this distance that requires work to be done, which results in an increase of the potential energy of the particle system. Hence, the attractive force between the particles is found by differentiation of χ with respect to ω.

In Fig. 5, χ is plotted for four different values of Ψ, together with the result for rigid particles ($\eta = 0$ for all

values of ζ). It is notable that for $\zeta < 0.6368$ all five curves merge into the same steepest slope, indicating that at this point the maximum attractive force (or cohesion) is reached irrespective of the hardness of the solid.

MODEL OF BED ELASTICITY

When the gas velocity through a homogeneous bed is increased, the bed expands as long as the gas velocity is below the critical velocity at the bubble
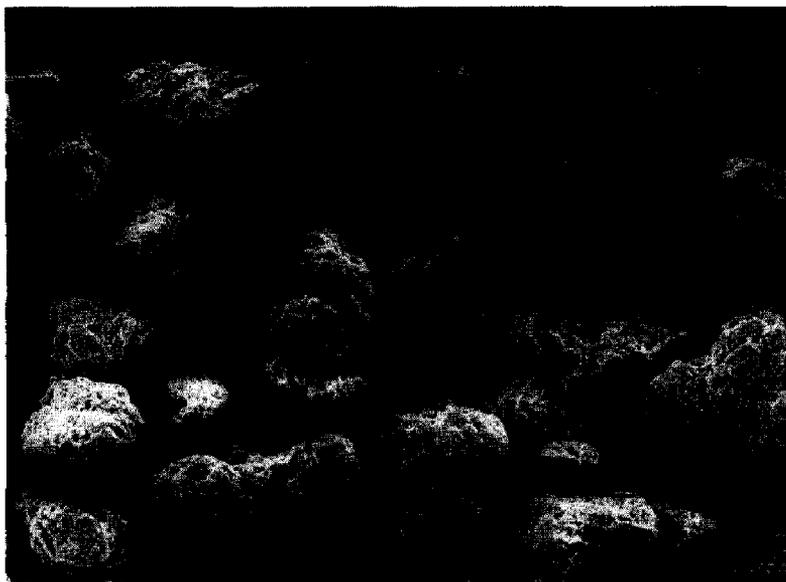
(c)

(d)

Fig. 3. Photographs of four powders: (a) spent cracking catalyst, magnification 310 ×; (b) fresh cracking catalyst, magnification 310 ×; (c) polypropylene, magnification 303 ×; (d) potato starch, magnification 860 ×.

point. This expansion, however, does not occur continuously but happens in small steps. During each step, the elasticity modulus is constant, but when the expansion becomes too large the elasticity limit of the bed is exceeded and some contact points between the powder particles will be broken. The powder bed then seeks a new structure with a somewhat higher porosity, with less contact points and with a new but lower elasticity modulus. On the other hand, when the gas

velocity is decreased, the drag force on the particles is decreased and the equilibrium between the drag force and the weight of the particles is disturbed. As long as the deviation of the equilibrium is not too large, it can be compensated for by the elastic force. When, however, the deviation becomes too large, the elasticity limit is exceeded and the powder structure seeks to rearrange itself and forms new contact points between the particles, now at a lower porosity. At the same
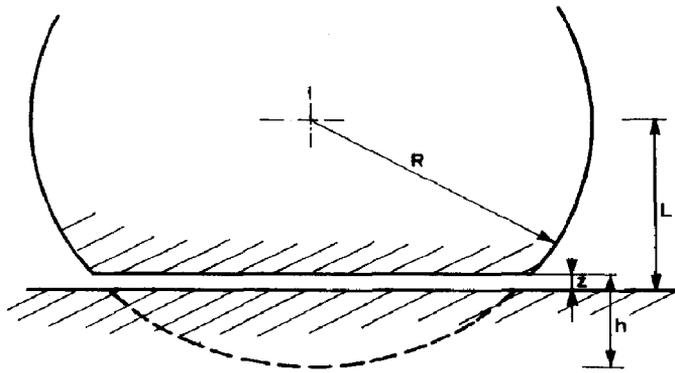
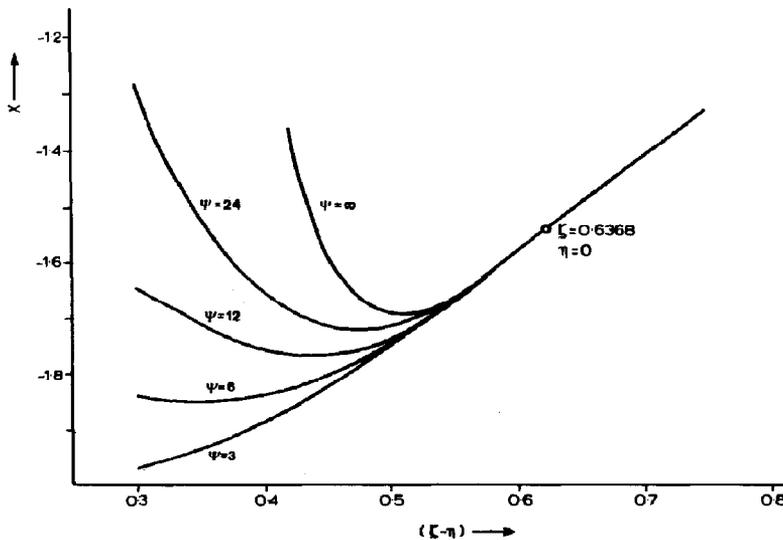Fig. 4. The geometry of a flattened particle adhering to a plane.

Fig. 5. Plot of dimensionless interaction potential between the deformed particles vs $\omega = \zeta - \eta$ ($\Psi = 3, 6,$ 12, 24). Comparison with rigid particles ($\eta = 0$).

time, the elasticity modulus of the powder bed increases. Hence, it can be concluded that there must be a direct relation between the elasticity modulus and the coordination number on one hand and the porosity on the other hand.

The relation between elasticity and porosity

We will now define the elasticity modulus of a homogeneous powder as follows. Suppose, we consider a small cube of powder with a porosity ε which consists of n layers of n^2 particles. We suppose that this powder cube has elastic properties. This means that when we apply a certain stress, σ_e, which is not too high, this causes a change $\Delta\varepsilon$ of the porosity of the cube, while this porosity change is entirely undone when the stress is taken away. Hence, the relation between the porosity change and the stress is perfectly

reversible. The elasticity modulus is now defined by

$$E = \frac{\sigma_e}{\Delta\varepsilon}. \tag{15}$$

Each layer of the powder cube has a thickness λ, which is increased with an amount $\Delta\lambda$ when the porosity is increased by an amount $\Delta\varepsilon$. From a mass balance it follows that

$$\Delta\varepsilon = (1 - \varepsilon)n\Delta\lambda. \tag{16}$$

The increase of the porosity is achieved by a force, F_λ, which operates at each contact point between the particles. It follows that

$$\sigma_e = n^2 F_\lambda \frac{k}{2} \tag{17}$$

in which k is the coordination number. The factor 2

comes in because each contact point is counted twice. With

$$n = \left(\frac{6(1 - \varepsilon)}{\pi d_p^3}\right)^{1/3} \tag{18}$$

it can be derived that

$$E = \frac{F_\lambda}{\Delta \lambda} \frac{k}{2d_p} \left(\frac{6}{\pi(1 - \varepsilon)^2}\right)^{1/3} \tag{19}$$

When the stress is not too high, the ratio $F_\lambda/\Delta\lambda$ may be assumed to be independent of the porosity. When it is taken into account also that the coordination number k is a separate function of the porosity, the porosity dependence of the elasticity is given by

$$\frac{E}{E_0} = k(1 - \varepsilon)^{-2/3} \tag{20}$$

in which E_0 is some reference number.

The coordination number

The coordination number is defined as the number of contacts which an average particle has with neighbouring particles in a regular and homogeneous packing. It will be clear that this coordination number will strongly depend on the porosity of the packing, while also a spread in particle size and the cohesion will affect this number. In his thesis Vervoorn (1977) gives a survey of the results and relations on the subject found in literature.

Following Smith [see Manegold (1955)], Rumpf (1958) suggested that a practical relation is given by $k\varepsilon = 3.1$. This relation, however, cannot hold, of course, for $\varepsilon \to 1$ since in that case k must go to zero. It can even be argued that $k = 2$ must be an absolute minimum since in a coherent and regular packing the limit is reached when the particles are stacked upon each other without any sideward support.

Consequently, it is not clear how in the literature results can be presented which should hold for $\varepsilon \to 1$. We will introduce here

$$k^* = k - 2. \tag{21}$$

We consider a cube of N particles with volume V_p. The total number of contacts in this cube is $N_c = Nk/2$. The total pore volume in the cube is

$$V_\varepsilon = NV_p \frac{\varepsilon}{1 - \varepsilon}. \tag{22}$$

Suppose now that one contact point is broken as a result of the stress tensor operating on the cube of powder. The total pore volume of the powder will then increase with an amount ΔV_ε. The total volume of the powder will also increase with this amount, while the porosity is increased with $d\varepsilon$. It can be expected that ΔV_ε is related directly to the volume of one particle and will be inversely proportional to k^*. Hence, we assume that

$$(\Delta V_\varepsilon) = \gamma V_p/k^* \tag{23}$$

in which γ is a numerical constant. When $-dN_c$

contacts are broken (dN_c is negative!), the increase of the total pore volume must be

$$-(\Delta V_\varepsilon)\,dN_c = \frac{d}{d\varepsilon}(V_\varepsilon)\,d\varepsilon = \frac{NV_p}{(1 - \varepsilon)^2}\,d\varepsilon. \tag{24}$$

After substitution of eq. (23) and with $dN_c = Ndk/2$, it follows that

$$-\gamma \frac{dk}{2(k - 2)} = \frac{d\varepsilon}{(1 - \varepsilon)^2}. \tag{25}$$

Integration now gives

$$-\frac{\gamma}{2}\ln(k - 2) = \frac{1}{1 - \varepsilon} + C \tag{26}$$

in which C is an integration constant.

We now return to eq. (20) but replace k by k^*. This is justified by the following reasoning. Consider three pairs of contacting particles as they occur in a random packing. The three configurations a, b and c (see Fig. 6) will all be subjected to the same vertical stress. In the configuration a the increase of the vertical distance L caused by this stress cannot be more than the maximum increase $r_{ss}\Delta\omega$ as long as the contact between the particles is not broken (see Effect of particle deformation section). It has, therefore, practically no effect on the relation between F_λ and $\Delta\lambda$. By replacing k by k^*, these contacts are further excluded from the derivations.

We now assume that we have done two different experiments with the same powder but fluidized this powder with two different gases. For both experiments 1 and 2 the porosity and the elasticity modulus can be determined. Hence, from these experiments the ratio k_1^*/k_2^* can be derived with the help of eq. (20). Applying eq. (26) twice yields the following relation from which γ can be calculated:

$$\gamma = 2\left(\frac{1}{1 - \varepsilon_1} - \frac{1}{1 - \varepsilon_2}\right)\frac{1}{\ln(k_2^*/k_1^*)}. \tag{27}$$

The constant C can be determined only by trial and error.

The above analysis was applied to the results obtained with fresh cracking catalyst as a powder and six different gas combinations. These results are given again in Table 1 but only those obtained at a pressure of 1 bar in order to be sure that gas adsorption does not play a role and that the reference elasticity modulus E_0 is the same for all the results obtained.
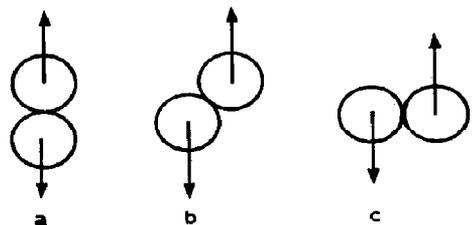

Fig. 6. Three configurations of two neighbouring particles.

Table 1. Relevant data of homogeneous fluidization of fresh cracking catalyst (FCC) with six different gases at 1 bar

Type of gas	ε_{mb}	u_{mb} (cm s^{-1})	E_{mb} (N m^{-2})
Hydrogen	0.511	0.80	0.850
Helium	0.578	0.57	0.293
Methane	0.538	0.70	0.560
Neon	0.617	0.50	0.182
Nitrogen	0.583	0.632	0.351
Argon	0.600	0.590	0.278

Table 2. The ratio k_1^*/k_2^* and the values of γ as derived for six gas combinations

Gas combination	k_1^*/k_2^*	γ
Argon–methane	0.451	0.842
Neon–hydrogen	0.182	0.664
Nitrogen–methane	0.585	0.854
Neon–nitrogen	0.490	0.596
Argon–nitrogen	0.286	0.728
Helium–hydrogen	0.298	0.536

The results of the calculations are presented in Table 2. The average value of γ was determined to be 0.704. When we assume that, on average, $k^* = 6$ at $\varepsilon = 0.40$, this yields, with the above value of γ, for the constant C a value of -2.297. With these data, the theoretical curve of E/E_0 vs ε is as shown in Fig. 7. The empirical curve of E/E_0 vs ε as determined in Part I of this series and which runs

$$\frac{E}{E_0} = \frac{E_{50}}{E_0} e^{-15(\varepsilon - 0.50)} \qquad (28)$$

is plotted as well. This figure shows that the strong dependence of the elasticity modulus on the porosity can be well explained by the theory presented here [see also Rietema (1991)].

The origin of the elasticity

The elasticity of the powder structure is the result of concerted action of mechanisms which operate at different scales in the packing:

(1) At the scale of neighbouring molecules works the elasticity which is a consequence of the Lennard-Jones potential and which is a result of the dynamic equilibrium between an attractive and a repulsive force.

(2) At the scale of neighbouring particles an elasticity results from the integration of mechanism 1 over all molecules around the contact place of the particles.

(3) Also at the scale of neighbouring particles results an elasticity which is a consequence of elastic deformation of the particles.

(4) Where the real contact between the particles is by the presence of asperities, elastic deformation of these asperities results finally in a real packing elasticity.

This mechanism will be elaborated now for a pair of particles which contact each other in a configuration which is some average of the configurations b and c. It is assumed that the real contact is through two asperities (shown exaggerated in Fig. 8), although, in practice there will be often more than two.

The distance between the asperities is put equal to $2l$. As a result of the external force one of these asperities will be lengthened by Δy while the other will be compressed by the same amount. Following the theory (see Effect of particle deformation section), y is put equal to $z - h = r_{ss}\omega$. Owing to this mechanism the contact angle between the two particles will
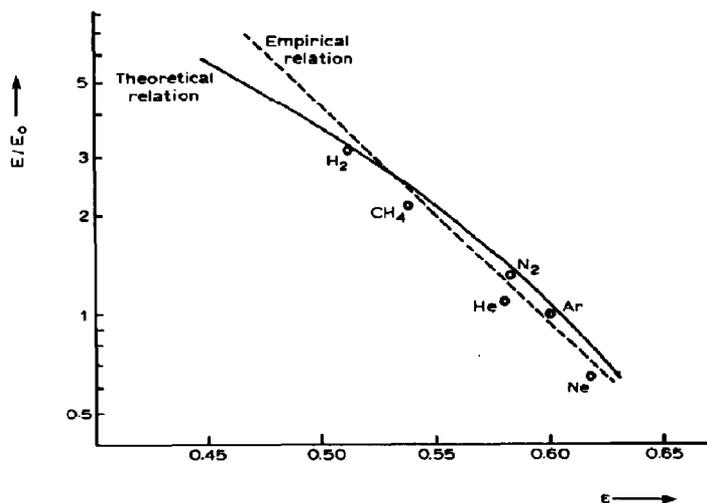

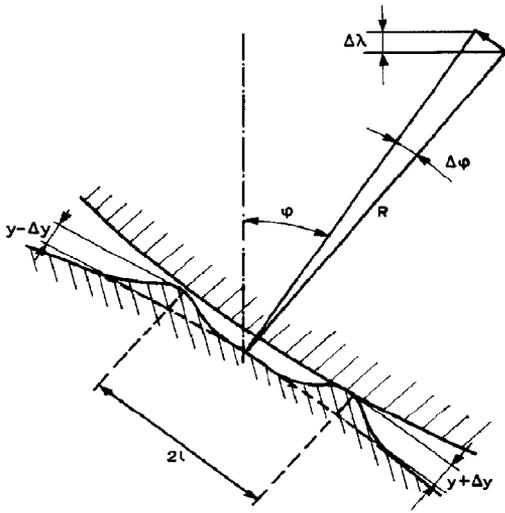Fig. 7. E/E_0 vs the porosity: empirical and theoretical relations.

Fig. 8. Schematic diagram of contact between two particles via asperities.

change by $\Delta\varphi$ and the vertical distance by $\Delta\lambda$. With $\Delta\varphi = \Delta y/l$ it follows that $\Delta\lambda = (R/l)\Delta y \sin\varphi$. Averaged over all possible configurations,

$$\overline{\Delta\lambda} = \frac{\pi R \, \Delta y}{4l}. \qquad (29)$$

The moment M_λ exerted on the particles by the external force is $F_\lambda d_p \sin\varphi$.

Averaged over all configurations

$$\bar{M}_\lambda = (\pi/4)F_\lambda d_p.$$

The moment exerted by two asperities is

$$M_y = 2lF_y.$$

These two moments must be equal; hence,

$$F_\lambda = \frac{8l}{\pi d_p} F_y. \qquad (30)$$

Substitution of eqs (29) and (30) into eq. (19) gives

$$E = \frac{32l^2}{\pi^2 d_p^3} k^* \left(\frac{F_y}{\Delta y}\right) \left[\frac{6}{\pi(1-\varepsilon)^2}\right]^{1/3}. \qquad (31)$$

F_y can be calculated from eq. (9) with a value $\Phi = 1.85$, which holds for the maximum external force without breaking the contact:

$$\Phi = \frac{6r_{ss}^2 F_y}{A R_a}.$$

In this equation R_a is now the radius of an asperity.

When for the relevant powder the parameter $\Psi = 12$, the maximum decrease in the flattening of the asperities amounts to $\Delta y = 0.2 r_{ss}$ (see Fig. 5). Hence, it can be derived that

$$\frac{F_y}{\Delta y} = \frac{1.54 A R_a}{r_{ss}^3}. \qquad (32)$$

When we assume that the porosity $\varepsilon = 0.5$, then from

eq. (26) it follows that $k^* = 2.325$. With $d_p = 60 \ \mu$m, $A = 10^{-19}$ J and $r_{ss} = 3.5 \times 10^{-10}$ m it is found that

$$E = 0.25(l^2 R_a)10^{24} \ \text{N m}^{-2} \qquad (33)$$

The result found for E is strongly determined by the choice made for l and R_a. Unfortunately, there is not enough information available on the distribution of the asperities over the surface of the particles and this information will be difficult to obtain.

With a choice of $l = 200$ Å and $R_a = 100$ Å, it is found that $E = 1.0$ N m^{-2}, which at least is of the right order of magnitude. It is believed, therefore, that on the basis of the model presented, it is possible to explain the values of E as derived from the experiments discussed in Part I of this series. Nevertheless, any result for E on the basis of assumptions about l and R_a are as yet purely speculative.

According to Rumpf (1958) [see also Molerus (1975)], the tension cut-off σ_c is given by

$$\sigma_c = \frac{kF_y}{\pi d_p^2} (1 - \varepsilon). \qquad (34)$$

It must be remarked that in this equation k should not be replaced by k^* as particles in configuration a (see Fig. 6) certainly make a strong contribution to the tension cut-off. After substitution of eq. (34) into eq. (31), we find for the ratio E/σ_c

$$E/\sigma_c = 12.6 \left(\frac{k-2}{k}\right) \left(\frac{l^2}{\Delta y d_p}\right)(1-\varepsilon)^{-5/3}. \qquad (35)$$

With $l = 200$ Å, $\Delta y = 1$ Å and $d_p = 50 \ \mu$m as an example, the dependence of E/σ_c on the porosity is shown in Table 3. A notable point in this table is that at not too high a porosity the ratio E/σ_c does not differ too much from 1.

INFLUENCE OF GAS ADSORPTION ON INTERPARTICLE FORCES

Several investigators (Subzwari et al., 1978; Abrahamsen and Geldart, 1980; Guedes de Carvalho, 1981) have found that fluidization at higher gas pressures can have a favourable effect on fluidization behaviour, as demonstrated by increased bed height and smaller gas bubbles. This is remarkable as the particle size and the particle density are constant. Indeed, the gas density increases with the gas pressure

Table 3. The theoretical coordination number k and the ratio of the elasticity modulus E to the cohesion constant σ_c as a function of the porosity ε

ε	k	E/σ_c
0.40	8	1.77
0.45	5.897	1.80
0.50	4.325	1.72
0.55	3.237	1.46
0.60	2.577	1.04
0.65	2.204	0.54

but is so much smaller than the solid density that it can hardly explain any effect on the fluidization behaviour. Finally, also the gas viscosity is practically independent of the gas pressure.

To solve this seeming contradiction, Rietema and Mutsers (1978) suggested that increased gas adsorption onto the surface of the solid particles could explain the phenomena found. According to these authors the interparticle forces will increase with pressure and, thus, cause an increase of the elasticity modulus. It was found, indeed, that an increase of the amount of gas adsorbed to the surface of the solid particles has the consequence that the cohesion between the particles is increased (Piepers et al., 1984).

A fundamental analysis of the effect of gas adsorption was carried by Cottaar and Rietema (1986). From this analysis it follows that indeed gas adsorption can indeed cause an increase of interparticle forces. A rigorous treatment of this analysis is beyond the scope of this paper. For such a treatment the reader is referred to Cottaar and Rietema (1986) and Rietema (1991).

CONCLUSIONS

A stable homogeneous bed of fine, more or less uniform, solid particles forms a mechanical structure, also when fluidized by gas. Of such a bed, elasticity is a real and essential property which determines the dynamic behaviour of the bed. The origin of this elasticity is to be found in the van der Waals forces which the solid particles exert upon each other. The strength of elasticity can be easily determined from simple homogeneous fluidization experiments [eq. (1)].

A theoretical model of the bed structure has been developed which explains the effect of the various properties of the involved particle phase. This model is composed of two sub-models:

(a) a simple model which describes the strong dependence of the coordination number on the porosity, and

(b) a rather complicated model which describes the dependence of the elasticity modulus on the size and surface distribution of the surface asperities.

NOTATION

A	Hamaker constant, N m
C_{ss}	constant in Lennard-Jones potential, J m^6
d_p	particle diameter, m
D	equivalent diameter of contacting particles, m
E	elasticity modulus, N m^{-2}
F	force between particles, N
F_c	cohesion force, N
F_y	elastic force at asperity contact, N
F_λ	force at the particle contact, N
h	flattening of the particles, m
k	coordination number, dimensionless
K	$=(1-v^2)/Y$, N^{-1} m^2

L	distance between the particle centre and the surface of the plane, m
l	distance between the two asperities, m
M_y	moment exerted on the particles, N m
M_λ	moment exerted by the asperities, N m
$n_{1,2}$	molecule density, m^{-3}
n	number of particles per unit length of powder packing, m^{-1}
N	number of particles in volume V, dimensionless
N_c	number of particle contacts in volume V, dimensionless
r	distance between the molecules, m
r_{ss}	molecule parameter, m
R	radius of the particle, m
R_a	radius of an asperity, m
u_0	superficial velocity, m s^{-1}
U	total potential of the system, J
U_h	potential of elastic deformation, J
U_m	total molecular potential of the system, J
$V_{1,2}$	volume elements of interacting particles, m^3
V_p	volume of a particle, m^3
V_{ss}	intermolecular potential, J
V_ϵ	total pore volume in volume V, m^3
Y	Young's modulus of elasticity, N m^{-2}
z	smallest distance between the particles, m

Greek letters

γ	proportionality constant, dimensionless
ε	porosity, dimensionless
ζ	dimensionless distance, dimensionless
η	dimensionless flattening, dimensionless
λ	thickness of a layer of particles
v	Poisson's ratio, dimensionless
ρ_p	particle density, kg m^{-3}
σ_c	cohesion constant, N m^{-2}
σ_e	stress operating on the packing, N m^{-2}
Φ	dimensionless force, dimensionless
χ	dimensionless interaction energy, dimensionless
Ψ	dimensionless elastic deformation energy, dimensionless
ω	$=\zeta-\eta$, dimensionless

REFERENCES

Abrahamsen, A. R. and Geldart, D., 1980, Behaviour of gas fluidized beds of fine powders. Part I. Homogeneous expansion. *Powder Technol.* **26**, 35.

Boehme, G., Krupp, H., Rabenhorst, H. and Sandstede, G., 1962, Adhesion measurements involving small particles. *Trans. Inst. Chem. Engrs* **40**, 252.

Bradley, R. S., 1932, On the cohesive forces between solid surfaces and the surface energy of solids. *Phil. Mag.* **13**, 853.

Cottaar, E. J. E. and Rietema, K., 1986, A theoretical study on the influence of gas adsorption on interparticle forces in powders. *J. Colloid Interface Sci.* **109**, 249.

Dahneke, B., 1972, The influence of flattening on the adhesion of particles. *J. Colloid Interface Sci.* **40**, 1.

Derjaguin, B. V., Muller, V. M. and Toporov, Y. P., 1975, Effect of contact deformations on the adhesion of particles. *J. Colloid Interface Sci.* **53**, 314.

Donsi, G. and Massimilla, L., 1973, Particle to particle forces in fluidization of fine powders, in *Proceedings of the*

International Symposium on Fluidization and Its Applications, p. 41. Toulouse, France.

Guedes de Carvalho, J. R. F., 1981, Dense phase expansion in fluidized beds of fine particles. The effect of pressure on bubble stability. *Chem. Engng Sci.* **36**, 413.

Hamaker, H. C., 1937, The London–van der Waals attraction between spherical particles. *Physica* **4**, 1058.

Hertz, H., 1895, *Gesammelte Werke*. Leipzig, Germany.

Johnson, K. L., Kendall, K. and Roberts, A. D., 1971, Surface energy and the contact of elastic solids. *Proc. Roy. Soc. Lond.* A**324**, 301.

Krupp, H., 1967, Particle adhesion, theory and experiment. *Adv. Colloid Interface Sci.* **1**, 941.

Lennard-Jones, J. E., 1937, The equation of state of gases and critical phenomena. *Physica* **4**, 941.

Lifshitz, E. M., 1956, *Sov. Phys.* **2**, 73.

London, F., 1937, The general theory of molecular forces. *Trans. Faraday Soc.* **33**, 8.

Manegold, E., 1955, *Kapillar Systeme*, Vol. 1. Strassenbahn Chemie und Technik, Heidelberg, Germany.

Massimilla, L. and Donsi, G., 1976, Cohesive forces in fluidization of fine particles. *Powder Technol.* **15**, 253.

Molerus, O., 1975, Theory of yield of cohesive powders. *Powder Technol.* **12**, 259.

Piepers, H. W., Cottaar, E. J. E., Verkooyen, A. H. M. and Rietema, K., 1984, Effects of pressure and type of gas on particle–particle interaction and the consequences for gas

solid fluidization behaviour. *Powder Technol.* **37**, 55.

Pollock, H. M., 1978, Contact adhesion between solids in vacuum. II. Deformation and interfacial energy. *J. Phys. D: Appl. Phys.* **11**, 39.

Rietema, K. and Mutsers, S. M. P., 1978, The effect of gravity upon the stability of a homogeneously fluidized bed, investigated in a centrifugal field, in *Fluidization* (Edited by J. F. Davidson and D. L. Keairns). p. 81. Cambridge University Press, Cambridge.

Rietema, K. and Piepers, H. W., 1990, The effect of inter-particle forces on the stability of gas-fluidized beds—I. Experimental evidence. *Chem. Engng Sci.* **45**, 1627.

Rietema, K., 1991, *The Dynamics of Fine Powders*. Elsevier, London.

Rumpf, H., 1958, Grundlagen und Methoden des Granulierens. *Chemie-Ingr-Tech.* **30**, 144.

Subzwari, M. P., Clift, R. and Pyle, D. L., 1978, Bubbling behaviour of fluidized beds at elevated pressure, in *Fluidization* (Edited by J. F. Davidson and D. L. Keairns), p. 50. Cambridge University Press, Cambridge.

Tabor, D., 1977, Surface forces and surface interactions. *J. Colloid Interphase Sci.* **58**, 2.

Vervoorn, P. M. N., 1977, Ph.D. thesis, Delft University of Technology, The Netherlands.

Visser, J., 1972, On Hamaker constants. A comparison between Hamaker constants and Lifshitz–van der Waal constants. *Adv. Colloid Interface Sci.* **3**, 331.